ACS Photonics

Article

pubs.acs.org/journal/apchd5

Optical Trapping and Two-Photon Excitation of Colloidal Quantum Dots Using Bowtie Apertures

Russell A. Jensen,[†,‡] I-Chun Huang,[†,§] Ou Chen,[‡] Jennifer T. Choy,[§] Thomas S. Bischof,[‡] Marko Lončar,[*,§] and Moungi G. Bawendi[*,‡]

[‡]Department of Chemistry, Massachusetts Institute of Technology, Cambridge, Massachusetts 02139, United States

[§]John A. Paulson School of Engineering and Applied Sciences, Harvard University, Cambridge, Massachusetts 02138, United States

Supporting Information

ABSTRACT: We demonstrate bowtie apertures that were designed and fabricated by a lift-off process to optically trap individual, 30 nm, silica-coated quantum dots (scQD). Simulations and experiments confirm the trapping capability of the system with a relatively low continuous wave trapping flux of 1.56 MW/cm^2 at 1064 nm. Additionally, the scQD emits upon trapping via two-photon excitation from the trapping laser due to strong field enhancement inside the aperture. This system is an exciting platform for studying light−matter interactions and mulitphoton processes in single emitters.

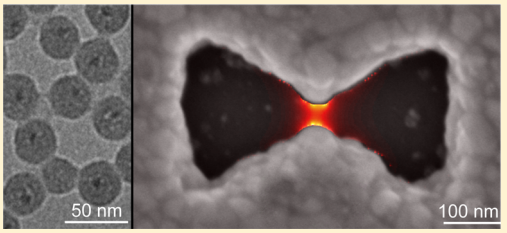

KEYWORDS: *optical trapping, two-photon, plasmonics, quantum dot, bowtie aperture*

Optical tweezers have been a powerful tool to fix, control, and manipulate small objects.[1] The introduction of plasmonic structures has further greatly advanced the field of optical trapping in the past decade. These structures provide enhanced, localized electric fields that require lower incident flux and can trap smaller particles when compared to free space trapping.[2−7] Trapping is further enhanced in plasmonic apertures by self-induced back-action (SIBA),[8] a positive feedback mechanism that increases the trapping force due to dielectic loading of the aperture when a particle is trapped. Recently, there have been many plasmonic nanoapertures designed for trapping particles as small as tens of nanometers. Trapping with plasmonic apertures has been performed with circular[8] and rectangular apertures.[9] Introducing a pinch point into the aperture, Pang and Gordon used double nanoholes to trap a 12 nm silica bead,[10] and Berthelot et al. fabricated bowtie apertures on films and on fiber tips to implement 20 nm polystyrene bead trapping and 50 nm bead manipulation.[11] The opposing prongs at the pinch point of the aperture act as dual sharp tips to greatly enhance electric fields in the gap,[12] giving rise to a localized field gradient suitable for optical trapping. This confined fundamental gap mode has also been used to provide a narrower near-field pattern for lithography,[13] higher throughput near-field scanning optical microscopy,[14] and enhanced molecule fluorescence.[15]

Various types of particles have been used in optical trapping studies, including gold nanoparticles,[16] nanorods,[17−19] globular proteins,[20] single-cell organisms,[4,21] polystyrene spheres with[11] and without emissive dye,[10] and colloidal quantum dots (QDs).[22,23] Colloidal quantum dots (QDs) are attractive candidates for optical trapping and simultaneous electronic excitation because their high index of refraction[24] increases the trapping force, and their broad continuum of excited states makes them strong absorbers.[25,26]

Colloidal QDs have exciting applications in biomolecule labeling due to a high photobleaching threshold, good chemical stability, and tunable spectral properties. The ability to optically manipulate QDs may help in fluorescent marker placement and molecular force measurements, but fluxes required for optical trapping[22] and nonlinear excitation[23,27] in free space are large and may be harmful to biological samples. Plasmonics can help to decrease the required trapping power, but trapping with a plasmonic structure generally renders QDs nonemissive due to interactions with the nearby metal.[28,29] In this work, these issues were solved by trapping silica coated quantum dots (scQDs) using bowtie apertures in a silver film. The bowtie apertures facilitated optical trapping and two-photon excitation such that the required flux was over 1 order of magnitude lower than previously reported for trapping in free space,[23] and the silica coating insulated the QDs from the metal to mitigate quenching. Also, the bowtie apertures were fabricated by e-beam lithography followed by lift-off rather than the past conventional foused ion beam milling procedure to provide larger aperture quantities for higher throughput device testing.

Bowtie apertures were used to trap single silica-coated quantum dots (scQD) with a diameter of 30 nm with a trapping laser intensity of 1.56 MW/cm^2 at 1064 nm. Because of the strong field confinement inside the bowtie aperture, 640 nm scQD emission was detected following two-photon excitation by the 1064 nm trapping laser. The enhanced two-photon excitation eliminates the need for a separate excitation

Received: October 8, 2015
Published: January 25, 2016

DOI: 10.1021/acsphotonics.5b00575
ACS Photonics 2016, 3, 423−427

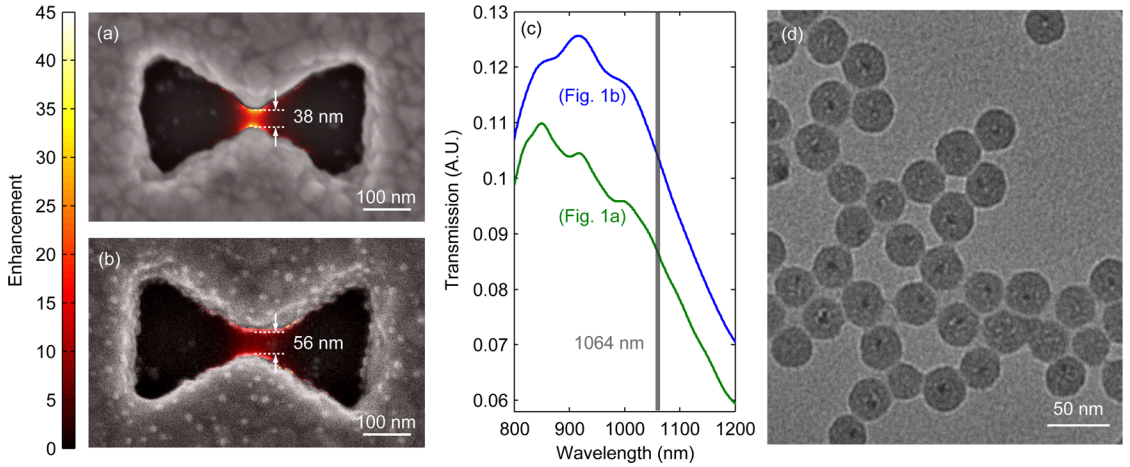

Figure 1. (a, b) SEM images of the bowtie apertures used in the experiments, overlapped with field intensity enhancement profiles at 1064 nm. The confined gap mode is dominant when the polarization is across the gap. (c) The simulated transmission spectra of the two apertures used in trapping experiments, showing peak resonances are blue-shifted from the 1064 nm trapping laser. (d) Transmission electron microscope image of the silica-coated quantum dots used in trapping.

source and results in a system that self-reports via emission when trapping is achieved. We show simulations to evaluate theoretical trapping performance and experimental examples of single scQD trapping with simultaneously recorded laser transmission and emission.

Scanning electron microscope (SEM) images of the apertures used in the experiments are shown in Figure 1a,b, overlapped with simulated field intensity enhancements. The dominant gap mode is supported by the aperture when the trapping beam polarization is oriented across the gap. Enhancement is a unitless factor that scales the intensity in the gap relative to the free space intensity. Both apertures, with gaps of 38 and 56 nm, were used to successfully trap scQDs. Given that the field enhancement is lower in the 56 nm gap aperture, the required trapping laser intensity is higher and the calculated trapping potential suggests it should only be able to trap larger particles (Supporting Information). The aperture is realized on an underlying silicon nitride (SiN) membrane (thickness 100 nm) and is immersed in water. A 3D sketch is provided in Supporting Information. In this way, the aperture forms a low-Q Fabry–Perot cavity whose resonance can be tuned by silver film thickness.[30] A 130 nm thick silver film was used to achieve resonances centered at 850 and 915 nm (Figure 1c). A transmission electron microscope (TEM) image of the scQDs used in trapping shows particles with a CdSe/CdS core/shell[31,32] center and total sizes that are ~30 nm in diameter (Figure 1d), with a mean hydrodynamic diameter of 39.2 nm as measured by dynamic light scattering (DLS, Supporting Information). Procedures for the fabrication of the bowtie apertures and synthesis of the scQDs are provided in Supporting Information.

It was shown in simulations that bowtie antennas might be able to tap a quantum dot, with the pumping wavelength near the resonance of the QD to create a larger dipole for easier trapping.[33] In order to quantify and evaluate the trapping capability of the apertures, finite-difference time-domain (FDTD) simulations (Lumerical Solutions, Inc.) were performed. Maxwell Stress Tensor was used to calculate the trapping force and then the force was integrated to get the trapping potential (Figure 2). Simulations were performed on the 38 nm gap aperture (Figure 1a) with the incident trapping beam focused on the entrance of aperture. The scQD was

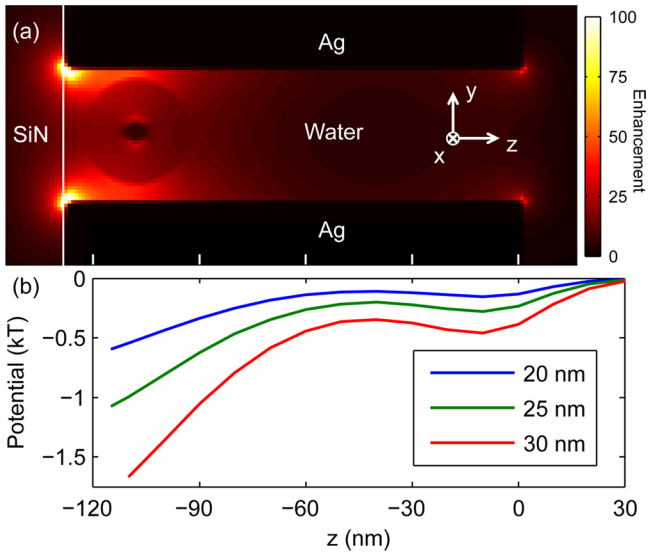

Figure 2. (a) Simulated field intensity distribution inside the aperture showing field enhancement on both faces of the aperture. The 30 nm scQD is shown in its final position at the bottom of the aperture touching the SiN membrane. (b) Potential energy calculation results showing that scQDs of at least 25 nm will have a potential lower than 1 k_BT at the bottom of the aperture.

simulated as a 6 nm CdSe core with silica coatings of varying thickness to produce final diameters of 20, 25, and 30 nm and was placed close to the silver wall to get the strongest trapping potential possible. The field intensity before entering the aperture was recorded, scaled to the experimental incident flux of 1.56 MW/cm^2, and used to calculate trapping potential. The calculated trapping potential exhibits two local minima due to field enhancement occurring on both faces of the aperture from operating near the first-order Fabry–Perot resonance,[30] with the deeper trapping potential at the water–SiN interface. Optical trapping is considered favorable when the trapping potential overcomes the ambient thermal energy k_BT (T = 300 K), which was observed for particles of at least 25 nm in this system at the water–SiN interface. The trapping potential at the front surface of the aperture did not overcome k_BT, regardless of particle size. From the simulations mentioned

DOI: 10.1021/acsphotonics.5b00575
ACS Photonics 2016, 3, 423–427

above, we assumed that the trapped scQD is located at the bottom of aperture, touching the silicon nitride membrane and the apex of the bowtie. However, as discussed in literature,[34] it is possible that the QD could move around due to Brownian motion. Factors not accounted for in the simulations could potentially enable trapping particles smaller than 25 nm with this system. As Tsuboi et al.[28] suggested, van der Waals forces between the particle and the surrounding aperture surfaces could facilitate trapping when potentials do not overcome k_BT of ambient thermal energy, and reduced degrees of freedom for particle motion inside the aperture should reduce the particle's kinetic energy, making escape from the aperture more difficult. The trap stiffness that a 20 nm scQD experiences inside the aperture was calculated to be 0.42 and 0.07 fN/nm/mW for the x and z directions, respectively (Supporting Information), which are comparable to stiffness measured for similar double nanohole structures[35] and are nearly 2 orders of magnitude larger than in the case of free-space trapping.[22,23]

Prior to trapping experiments, the aperture film was packaged with an aqueous scQD solution based on a procedure presented by Pang and Gordon.[10] A reservoir was made by cutting a 3 × 3 mm square from a 30 μm thick polydimethylsiloxane (PDMS) spacer on top of a 80 μm thick coverslip. Then, a small drop of scQD solution (0.07% w/v) was placed in the reservoir, and the aperture film was placed face down on top of the reservoir. A cross section of the sample packaging is shown in the inset of Figure 3. We can see that our

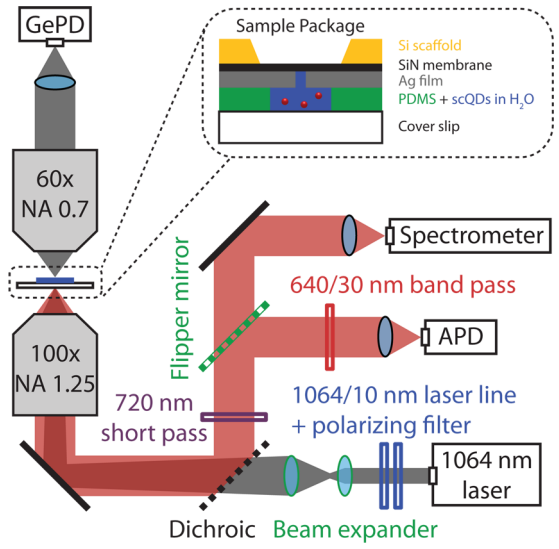

Figure 3. Instrument schematic for simultaneous trapping with 1064 nm laser (gray beam) and scQD emission detection at 640 nm (red beam). (Inset) Cross section of sample package.

aperture device is surrounded by silver with size of 7.5 × 7.5 mm square. Its high thermal conductivity (429 W/m/K) should act as a good heat sink. This implies that our device temperature should not increase too much under the trapping laser illumination.[6]

Optical trapping was achieved by transmitting a continuous wave (CW) 1064 nm trapping beam through an aperture packaged with scQDs, as shown in Figure 3. The optical quality of a 1064 nm trapping beam (Laser Quantum Ventus 1064) was cleaned with a polarizing filter and a 1064/10 nm laser line filter, expanded, and slightly defocused to correct for chromatic aberration of the trapping objective. The trapping objective was a 100× (1.25 NA) oil immersion objective that formed a spot radius of 1 μm with 1.56 MW/cm^2 of incident flux at 1064 nm. Emission from trapped scQDs was collected with the same objective, separated from the 1064 nm trapping beam with a 900 nm short pass dichroic mirror and sent to either a silicon avalanche photodiode (APD, PerkinElmer SPCM -AQRH-13) or a spectrometer/CCD camera combination (Princeton Instruments Acton SP2750A/Pixis 1024) for detection of two-photon excitation upon trapping. Above the packaged film, 1064 nm transmission intensity through the aperture was collected with a 60× (0.7 NA) air objective and sent to a Ge photodiode (Thorlabs DET50B) to monitor jumps in transmission intensity coinciding with trapping events. Sample positioning was achieved by a three-axis stage (Thorlabs Nanomax-TS).

Single scQD trapping in the 38 nm aperture using scQDs shown in Figure 1 is demonstrated in Figure 4 and is

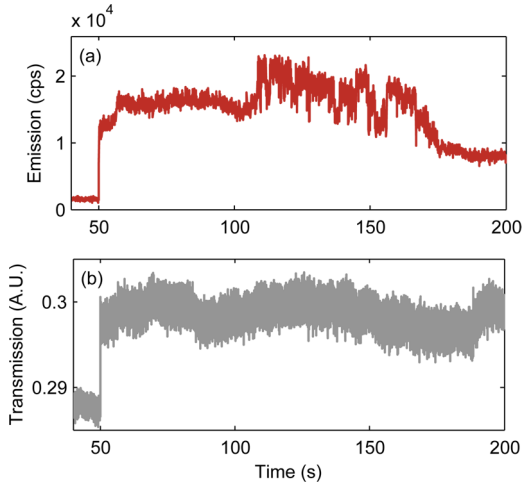

Figure 4. (a) Emission and (b) 1064 nm transmission channels show a stepwise increase in signal at 50 s, indicating individual scQD trapping.

characterized by a stepwise increase in both emission and transmission intensities at 50 s. Intensity fluctuations are observed in the emission channel at ∼110 s followed by a gradual decrease in intensity. Corresponding dynamics in the transmission channel are absent or undetectably small, suggesting that scQD emission dynamics (i.e., blinking, bleaching) may be responsible for the fluctuations observed in the emission channel. See Supporting Information for further examples of trapped scQD emission dynamics. Alternatively, the emission channel may be far more sensitive to very small changes in particle position due to the nonlinear nature of two-photon excitation, resulting in large fluctuations in the emission channel accompanied by an increase in transmission channel noise. This might also explain the measured signals at 60 and 160 s: there is a small increase followed by gradual decrease in the emission intensity, with no observable change in the transmission intensity. We believe that this can be explained by scQD moving into and then out of the location with stronger excitation flux. A final possibility is that two particles were simultaneously trapped and emission ensued for the respective particles at 50 and 110 s. This final scenario is unlikely, however, because trapping particles or clusters larger than the 38 nm gap is not expected. Large particles and clusters are prevented from peak trapping potentials at the bottom of the aperture.[10] In general, the trapping here was more of an one-off

DOI: 10.1021/acsphotonics.5b00575
ACS Photonics 2016, 3, 423−427

event, since we were using a size distribution of particles and a distribution of different bowtie shapes. Further optimization is required in order to make trapping routine.

Figure 5 shows spectra collected from the same aperture before and after scQD trapping and serves as evidence for two-photon excitation in the absence of a sub-bandgap excitation source. The spectral range between 520 to 700 nm is dark prior to trapping, but a scQD emission peak appears at 640 nm after the particle is trapped. Additionally, the absence of detected signal at 532 nm rules out second harmonic generation in the aperture by the trapping beam. The emission and transmission intensities for this trapping event are given in the Supporting Information, along with the scQD linear emission spectrum excited with a 532 nm CW excitation source. Given the simulated peak intensity enhancement of ~48× for this aperture with a scQD in the aperture (Figure 2a, the enhancement around the scQD not the corner), the enhanced excitation flux at the trapped scQD is calculated to be 74.9 MW/cm^2. This enhanced excitation flux, suitable for two-photon excitation of QDs,[23] can be reached with a very low incident flux of 1.56 MW/cm^2 at 1064 nm, due to the strong plasmonic enhancement provided by the aperture.[36] We note that the enhanced flux inside the aperture is a factor of five larger than the flux reported using free space trapping.[22]

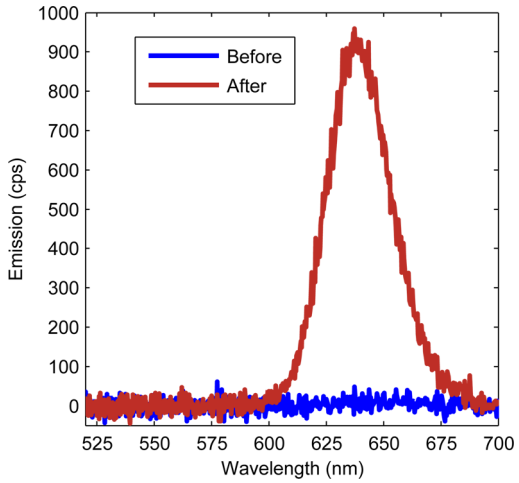

Figure 5. QD emission spectra before (blue) and after (red) optical trapping and two-photon excitation.

The system presented here offers unique opportunities to study light−matter interactions inside a plasmonic cavity.[37] In the experiments, scQDs did not stay inside the aperture after turning off the trapping laser, so the particle can be controllably placed and removed from the aperture by toggling the trapping beam, allowing for convenient measurements of the emitter inside and outside of the cavity. The optical trap also provides natural alignment of the nanoparticle to the peak field intensity in the aperture, alleviating concerns over particle placement in a resonant cavity,[38] and the lift-off nature of the aperture fabrication can enable fabrication of large arrays of apertures, each designed to operate at slightly different wavelength, allowing for high throughput cavity resonance optimization. When combined with our trapping based incorporation of QDs, this can eliminate the need for postfabrication cavity tuning and trimming: it is always possible to find and work with a resonator that is tuned to the emission wavelength of the emitter. Additionally, the platform might enable studies of individual QD absorption spectrum over wide wavelength range. This can be difficult using free-space approaches due to orders of magnitude difference between the absorption cross-section of the QD and the diffraction limited focal spot. This issue can be alleviated with our device due to the confined gap mode and the fact that aperture nature ensures that orders of more transmitted light interacts with QD trapped inside the aperture. Lastly, experiments need not be limited to scQDs. Emitter−cavity interactions can be investigated for alternative quantum emitters including nitrogen-vacancy centers in diamond,[39] semiconductor nanorods, and hybrid structures.[40]

In conclusion, bowtie apertures were designed and fabricated to optically trap 30 nm insulated QDs, yielding a system with stable single particle trapping and robust two-photon excitation at modest flux. Lift-off aperture fabrication was introduced and FDTD simulations revealed favorable trapping conditions that may be further aided by nonoptical mechanisms. This system may enable the high-throughput experimentation of light−matter interactions and multiphoton processes in various types of emitters.

■ ASSOCIATED CONTENT

Supporting Information

The Supporting Information is available free of charge on the ACS Publications website at DOI: 10.1021/acsphotonics.5b00575.

Silica-coated QD synthesis and characterization, aperture fabrication, 56 nm aperture trapping potential, trap stiffness calculations, trapped particle emission dynamics, and spectrally detected trapping event (PDF).

■ AUTHOR INFORMATION

Corresponding Authors

*E-mail: loncar@seas.harvard.edu.
*E-mail: mgb@mit.edu.

Author Contributions

†These authors contributed equally to this work (R.A.J. and I.-C.H.).

Notes

The authors declare no competing financial interest.

■ ACKNOWLEDGMENTS

Research supported as part of the Center for Excitonics, an Energy Frontier Research Center funded by the U.S. Department of Energy, Office of Science, Basic Energy Sciences (BES) under Award No. DE-SC0001088 (simulations, aperture fabrication, trapping experiments), and by the National Institutes of Health (NIH) under Award 5-U54-CA151884 (scQD synthesis). The authors thank Prof. Karl Berggren, Lisa Marshall, Shota Kita, and Cheng Wang for guidance and fruitful discussions.

■ REFERENCES

(1) Ashkin, A.; Dziedzic, J. M.; Bjorkholm, J. E.; Chu, S. Observation of a single-beam gradient force optical trap for dielectric particles. *Opt. Lett.* **1986**, *11*, 288−290.

(2) Righini, M.; Zelenina, A. S.; Girard, C.; Quidant, R. Parallel and selective trapping in a patterned plasmonic landscape. *Nat. Phys.* **2007**, *3*, 477−480.

(3) Grigorenko, A. N.; Roberts, N. W.; Dickinson, M. R.; Zhang, Y. Nanometric optical tweezers based on nanostructured substrates. *Nat. Photonics* **2008**, *2*, 365−370.

DOI: 10.1021/acsphotonics.5b00575
ACS Photonics 2016, 3, 423−427

(4) Righini, M.; Ghenuche, P.; Cherukulappurath, S.; Myroshnychenko, V.; García de Abajo, F. J.; Quidant, R. Nano-optical Trapping of Rayleigh Particles and Escherichia coli Bacteria with Resonant Optical Antennas. *Nano Lett.* **2009**, *9*, 3387−3391.
(5) Juan, M. L.; Righini, M.; Quidant, R. Plasmon nano-optical tweezers. *Nat. Photonics* **2011**, *5*, 349−356.
(6) Wang, K.; Schonbrun, E.; Steinvurzel, P.; Crozier, K. B. Trapping and rotating nanoparticles using a plasmonic nano-tweezer with an integrated heat sink. *Nat. Commun.* **2011**, *2*, 469.
(7) Tanaka, Y.; Kaneda, S.; Sasaki, K. Nanostructured potential of optical trapping using a plasmonic nanoblock pair. *Nano Lett.* **2013**, *13*, 2146−50.
(8) Juan, M. L.; Gordon, R.; Pang, Y.; Eftekhari, F.; Quidant, R. Self-induced back-action optical trapping of dielectric nanoparticles. *Nat. Phys.* **2009**, *5*, 915−919.
(9) Chen, C.; Juan, M. L.; Li, Y.; Maes, G.; Borghs, G.; Van Dorpe, P.; Quidant, R. Enhanced Optical Trapping and Arrangement of Nano-Objects in a Plasmonic Nanocavity. *Nano Lett.* **2012**, *12*, 125−132.
(10) Pang, Y.; Gordon, R. Optical Trapping of 12 nm Dielectric Spheres Using Double-Nanoholes in a Gold Film. *Nano Lett.* **2011**, *11*, 3763−3767.
(11) Berthelot, J.; Acimovic, S. S.; Juan, M. L.; Kreuzer, M. P.; Renger, J.; Quidant, R. Three-dimensional manipulation with scanning near-field optical nanotweezers. *Nat. Nanotechnol.* **2014**, *9*, 295−299.
(12) Novotny, L.; Hecht, B. *Principles of Nano-Optics*; Cambridge University Press, 2006.
(13) Wang, L.; Uppuluri, S. M.; Jin, E. X.; Xu, X. Nanolithography Using High Transmission Nanoscale Bowtie Apertures. *Nano Lett.* **2006**, *6*, 361−364.
(14) Mivelle, M.; van Zanten, T. S.; Neumann, L.; van Hulst, N. F.; Garcia-Parajo, M. F. Ultrabright bowtie nanoaperture antenna probes studied by single molecule fluorescence. *Nano Lett.* **2012**, *12*, 5972−8.
(15) Lu, G.; Li, W.; Zhang, T.; Yue, S.; Liu, J.; Hou, L.; Li, Z.; Gong, Q. Plasmonic-Enhanced Molecular Fluorescence within Isolated Bowtie Nano-Apertures. *ACS Nano* **2012**, *6*, 1438−1448.
(16) Hansen, P. M.; Bhatia, V. K.; Harrit, N.; Oddershede, L. Expanding the Optical Trapping Range of Gold Nanoparticles. *Nano Lett.* **2005**, *5*, 1937−1942.
(17) Pauzauskie, P. J.; Radenovic, A.; Trepagnier, E.; Shroff, H.; Yang, P.; Liphardt, J. Optical trapping and integration of semiconductor nanowire assemblies in water. *Nat. Mater.* **2006**, *5*, 97−101.
(18) Selhuber-Unkel, C.; Zins, I.; Schubert, O.; Sönnichsen, C.; Oddershede, L. B. Quantitative Optical Trapping of Single Gold Nanorods. *Nano Lett.* **2008**, *8*, 2998−3003.
(19) Head, C. R.; Kammann, E.; Zanella, M.; Manna, L.; Lagoudakis, P. G. Spinning nanorods - active optical manipulation of semiconductor nanorods using polarised light. *Nanoscale* **2012**, *4*, 3693−3697.
(20) Pang, Y.; Gordon, R. Optical Trapping of a Single Protein. *Nano Lett.* **2012**, *12*, 402−406.
(21) Ashkin, A.; Dziedzic, J. M.; Yamane, T. Optical trapping and manipulation of single cells using infrared laser beams. *Nature* **1987**, *330*, 769−771.
(22) Jauffred, L.; Richardson, A. C.; Oddershede, L. B. Three-Dimensional Optical Control of Individual Quantum Dots. *Nano Lett.* **2008**, *8*, 3376−3380.
(23) Jauffred, L.; Oddershede, L. B. Two-Photon Quantum Dot Excitation during Optical Trapping. *Nano Lett.* **2010**, *10*, 1927−1930.
(24) The index of refraction is 2.5367 at 1064 nm for bulk CdSe.
(25) Blanton, S. A.; Dehestani, A.; Lin, P. C.; Guyot-Sionnest, P. Photoluminescence of single semiconductor nanocrystallites by two-photon excitation microscopy. *Chem. Phys. Lett.* **1994**, *229*, 317−322.
(26) Larson, D. R.; Zipfel, W. R.; Williams, R. M.; Clark, S. W.; Bruchez, M. P.; Wise, F. W.; Webb, W. W. Water-Soluble Quantum Dots for Multiphoton Fluorescence Imaging in Vivo. *Science* **2003**, *300*, 1434−1436.
(27) Chiang, W.-Y.; Okuhata, T.; Usman, A.; Tamai, N.; Masuhara, H. Efficient Optical Trapping of CdTe Quantum Dots by Femtosecond Laser Pulses. *J. Phys. Chem. B* **2014**, *118*, 14010.
(28) Tsuboi, Y.; Shoji, T.; Kitamura, N.; Takase, M.; Murakoshi, K.; Mizumoto, Y.; Ishihara, H. Optical Trapping of Quantum Dots Based on Gap-Mode-Excitation of Localized Surface Plasmon. *J. Phys. Chem. Lett.* **2010**, *1*, 2327−2333.
(29) Zehtabi-Oskuie, A.; Jiang, H.; Cyr, B. R.; Rennehan, D. W.; Al-Balushi, A. A.; Gordon, R. Double nanohole optical trapping: dynamics and protein-antibody co-trapping. *Lab Chip* **2013**, *13*, 2563−2568.
(30) Ibrahim, I. A.; Mivelle, M.; Grosjean, T.; Allegre, J. T.; Burr, G. W.; Baida, F. I. Bowtie-shaped nanoaperture: a modal study. *Opt. Lett.* **2010**, *35*, 2448−2450.
(31) Chen, O.; Chen, X.; Yang, Y.; Lynch, J.; Wu, H.; Zhuang, J.; Cao, Y. C. Synthesis of Metal-Selenide Nanocrystals Using Selenium Dioxide as the Selenium Precursor. *Angew. Chem., Int. Ed.* **2008**, *47*, 8638−8641.
(32) Chen, O.; Zhao, J.; Chauhan, V. P.; Cui, J.; Wong, C.; Harris, D. K.; Wei, H.; Han, H.-S.; Fukumura, D.; Jain, R. K.; Bawendi, M. G. Compact high-quality CdSe-CdS core-shell nanocrystals with narrow emission linewidths and suppressed blinking. *Nat. Mater.* **2013**, *12*, 445−451.
(33) Dineen, C.; Reichelt, M.; Koch, S. W.; Moloney, J. V. Optical trapping of quantum dots in a metallic nanotrap. *J. Opt. A: Pure Appl. Opt.* **2009**, *11*, 114004.
(34) Jauffred, L.; Kyrsting, A.; Arnspang, E. C.; Reihani, S. N. S.; Oddershede, L. B. Sub-diffraction positioning of a two-photon excited and optically trapped quantum dot. *Nanoscale* **2014**, *6*, 6997−7003.
(35) Kotnala, A.; Gordon, R. Quantification of High-Efficiency Trapping of Nanoparticles in a Double Nanohole Optical Tweezer. *Nano Lett.* **2014**, *14*, 853−856.
(36) Wenseleers, W.; Stellacci, F.; Meyer-Friedrichsen, T.; Mangel, T.; Bauer, C. A.; Pond, S. J. K.; Marder, S. R.; Perry, J. W. Five Orders-of-Magnitude Enhancement of Two-Photon Absorption for Dyes on Silver Nanoparticle Fractal Clusters. *J. Phys. Chem. B* **2002**, *106*, 6853−6863.
(37) Farahani, J. N.; Pohl, D. W.; Eisler, H.-J.; Hecht, B. Single Quantum Dot Coupled to a Scanning Optical Antenna: A Tunable Superemitter. *Phys. Rev. Lett.* **2005**, *95*, 017402.
(38) Geiselmann, M.; Marty, R.; Renger, J.; Garcia de Abajo, F. J.; Quidant, R. Deterministic optical-near-field-assisted positioning of nitrogen-vacancy centers. *Nano Lett.* **2014**, *14*, 1520−5.
(39) Choy, J. T.; Bulu, I.; Hausmann, B. J. M.; Janitz, E.; Huang, I.-C.; Lončar, M. Spontaneous emission and collection efficiency enhancement of single emitters in diamond via plasmonic cavities and gratings. *Appl. Phys. Lett.* **2013**, *103*, 161101.
(40) Chen, O.; et al. Magneto-fluorescent core-shell supernanoparticles. *Nat. Commun.* **2014**, *5*, 5093.

DOI: 10.1021/acsphotonics.5b00575
ACS Photonics 2016, 3, 423−427